International Journal of Thermal Sciences 48 (2009) 1639–1648

Contents lists available at ScienceDirect

International Journal of Thermal Sciences

www.elsevier.com/locate/ijts

The influence of channel height on heat transfer enhancement of a co-angular type rectangular finned surface in narrow channel

M.D. Islam [a,*], K. Oyakawa [b], M. Yaga [b], I. Kubo [a]

[a] Department of Mechanical Systems Engineering, The Petroleum Institute, Abu Dhabi, P.O. Box 2533, United Arab Emirates
[b] Department of Mechanical Systems Engineering, Faculty of Engineering, University of the Ryukyus, 1 Senbaru, Nishihara, Okinawa 903-0213, Japan

ARTICLE INFO

Article history:
Received 21 April 2008
Received in revised form 13 January 2009
Accepted 13 January 2009
Available online 3 February 2009

Keywords:
Convective heat transfer
Height influence
Heat transfer enhancement
Infrared image system
Co-angular fin pattern

ABSTRACT

An experimental research was conducted to investigate the effect of channel height on heat transfer enhancement of a surface affixed with arrays (7×7) of short rectangular fins of a co-angular type pattern in channels. An infrared imaging system with the camera (TVS 8000) measured the temperature distributions to calculate the local heat transfer coefficients of the overall surface (fin base and endwall) of the representative fin regions. Heat transfer experiments were performed for a co-angular type fin pattern varying the channel to fin height ratio (H_d/H_f) from 2 to 5. Friction factors of the finned surfaces were calculated from pressure drop measurements. Relatively larger friction occurs for the smaller channel to fin height ratios and the friction factor slowly decreases with increasing Reynolds number. For the larger channel to fin height ratios, friction factor slowly increases with Reynolds number. The area averaged heat transfer decreases with increasing the channel to fin height ratio and channel aspect ratio, while heat transfer increases with the mainstream velocity. This is because, separation space between the channel wall and the fin top surface has a great influence on the phenomena of flow separated from the fin edge and vortex formation. At a smaller separation space, generated vortex is strongly reflected and vortex structure formation is adequately completed having full strength to interact with fins and endwall surface which leads to larger friction and contributes heat transfer enhancement. A detailed heat transfer analysis and iso-heat transfer coefficient contour gives a clear picture of the heat transfer characteristics of the overall surface. A relative performance graph indicates that the lowest channel to fin height ratio ($H_d/H_f = 2$) has the highest thermal performance out of the channels tested. In addition, significant thermal enhancement, 2.6–3 times the smooth surface value can be achieved at lower Reynolds numbers with a co-angular fin pattern in the channel.

1. Introduction

The recent development of more powerful chips and the miniaturization of electronic circuits and other compact systems have created a greater demand for development of efficient heat removal systems. Fins are widely used as the primary means of heat exchanging devices. With the increasing demand for high performance heat exchanging devices, researchers are now trying to use the fins as extended surfaces and, additionally, as vortex generators which is an emerging technology in the field of heat transfer. Recently, an inclined rectangular fin attached to the endwall is found to be an effective configuration for enhanced heat transfer, because the vortexes, longitudinal and other, produced by this fin maintain their intensity far downstream. It is expected that the heat transfer from the endwall and the fin surface can be improved and hence this configuration is identified as being very promising. The authors have conducted a series of experimental investigations [1–3] with rectangular fins, using different patterns and arrangements, to study heat transfer enhancement in a rectangular channel. The heat transfer enhancement in arrays of rectangular blocks in a channel has been investigated by other researchers. Sparrow et al. [4,5] studied the heat transfer and pressure drop characteristics of arrays of rectangular modules commonly encountered in electronic equipment and determined the thermal behavior of the arrays in different situations. Heat transfer enhancements exceeding a factor of two were achieved by using multiple fence like barriers, with the interbarrier spacing and the barrier height being varied parametrically with Reynolds number. Molki et al. [6] experimentally studied the heat transfer at the entrance region of an array of rectangular heated blocks and presented empirical correlations of the heat transfer for the array. Heat transfer from an array of parallel longitudinal fins to a turbulent air stream passing through the inter fin spaces has been investigated both numerically and experimentally by Kadle and Sparrow [7]. They found that the local heat transfer coefficients varied along the fins and along the

* Corresponding author.
E-mail address: mdislam02@yahoo.com (M.D. Islam).

1290-0729/$ – see front matter
doi:10.1016/j.ijthermalsci.2009.01.006

Nomenclature

A	cross sectional area of the channel	m^2	
D_H	hydraulic diameter of the channel	m	
f	friction factor		
L	fin length = 20 mm		
H_d	height of channel = 20–50 mm		
H_f	height of fin = 10 mm		
$\bar{h}$	area average heat transfer coefficient	$W/m^2\,K$	
h	heat transfer coefficient	$W/m^2\,K$	
h_x	streamwise local heat transfer coefficient	$W/m^2\,K$	
h_z	spanwise local heat transfer coefficient	$W/m^2\,K$	
$\overline{Nu}$	area-average Nusselt number ($\bar{h}D_H/\lambda$)		
$\dot{m}$	mass flow rate (ρAU)	kg/s	
P, P_∞	streamwise pressure and atmospheric pressure respectively	N/m^2	
t_w	wall temperature	°C	
t_∞	mainstream temperature	°C	
Re	Reynolds number (UD_H/ν)		
U	mainstream air velocity	m/s	
W	channel width = 230 mm		
X^*	streamwise coordinate ($X^* = 0$ at the center of rectangular fin of third row)		
Z^*	spanwise coordinate ($Z^* = 0$ at the center of rectangular fin of third row)		

Greek symbols

α	inclination angle	
ν	kinematic viscosity of air	m^2/s
λ	thermal conductivity	W/m K
ρ	density of air	kg/m^3

Subscripts

s	smooth surface
d	channel
f	fin

surface of the base plate. Turk and Junkhan [8] measured the spanwise heat transfer downstream of a rectangular fin mounted on a flat plate. El-Saed et al. [9] investigated heat transfer and fluid flow in rectangular fin arrays and found that the mean Nusselt number increases with increasing Reynolds number, inter-fin space and fin thickness but did not examine endwall heat transfer. Oyakawa et al. [10] studied the heat transfer of plate setting rectangular fins with an attack angle of 20° and showed that this configuration can enhance heat transfer. Igarashi [11] studied heat transfer from a square prism with different attack angles and observed reattachment flow for attack angles of 14°–35°. Bilen and Yapici [12] investigated heat transfer enhancement from a surface fitted with rectangular blocks at different attack angle and found that the maximum heat transfer was obtained at an angle of 45°, though the local heat transfer characteristics were not reported.

Some of the researchers also studied heat transfer enhancement considering the influence of the rectangular channel dimensions. Park et al. [13] studied heat transfer performance comparisons of five different rectangular channels with parallel angled ribs. In their research they investigated the combined effects of the channel aspect ratio, rib angle of attack and flow Reynolds number on heat transfer and pressure drop in rectangular channels. Their results showed that the narrow aspect ratio channel give much better heat transfer performance than the wide aspect ratio channels. Warrier et al. [14] performed heat transfer and pressure drop experiments in five parallel small rectangular channels. They varied the mass flow rate, inlet liquid sub cooling, and heat flux. Based on the measured temperatures, pressure drops and the overall energy balance across the test section, they calculated the heat transfer coefficients for both single phase forced convection and flow boiling. They developed a correlation for two phase flow pressure drop under sub cooled and saturated nucleate boiling condition. Mingoo and Keumnam [15] also investigated the effect of aspect ratio of rectangular channels on the cooling characteristics of paraffin slurry flow. They observed that the influence of the aspect ratio of the rectangular channel on the local heat transfer coefficients for both water and paraffin slurry at a high heat flux was greater than at low heat flux.

Chang et al. [16] studied the influence of channel height on heat transfer in rectangular channels with skewed ribs at different bleed conditions. They calculated average heat transfer and thermal performance factors to establish the heat transfer correlations with applications to the design of coolant channels in a gas turbine blade. In the other research, Chang et al. [17] experimentally studied heat transfer and pressure drop in a rectangular narrow channel roughened by scaled surfaces on two opposite walls. Experimental correlations of heat transfer and friction coefficient were derived for the scale roughened rectangular channel. Murata and Mochizuki [18] studied the effect of cross-sectional aspect ratio on turbulent heat transfer in an orthogonally rotating rectangular duct with angled rib turbulators. In their study heat transfer was numerically simulated where the rotation number and the duct aspect ratios were varied for a friction Reynolds number of 350 and rib angle of 60°. They showed how local heat transfer was changed by duct aspect ratio.

As the above literature review shows, previous studies have investigated heat transfer enhancement from surfaces in rectangular channels and a few studies only have concentrated on heat transfer considering channel aspect ratio. Very few studies are found dealing research with the effect of channel height on the heat transfer from the arrays of rectangular finned surface in channels. Therefore, we have investigated the influence of channel height on the heat transfer enhancement and friction factor for short rectangular fins on a channel wall, because the separation space between the channel wall and fin top edge has a great influence on the formation of vortex structure and flow behavior. In smaller channel to fin height ratio, vortex generated by the inclined fin is reflected by the lower wall that strongly touches the endwall and fin surfaces which increase the friction. On the other hand, at larger channel to fin height ratio, the lower wall has comparatively less influence on the vortex structure and the flow is not reflected strongly by the wall as well. So less friction is experienced. Both strength and circulation of the vortex structure are affected by the lower wall of the channel which contributes heat transfer enhancement.

This paper attempts to analyze the detailed heat transfer characteristics of overall surface for the co-angular type fin pattern. Detailed heat transfers as well as averaged heat transfer coefficients are estimated from the infrared image of the representative fin region for different channel to fin height ratios and the channel aspect ratios.

2. Experimental apparatus and procedure

Experiments were conducted in a long rectangular channel of 230 mm span (width) and 784 mm length. The channel height was varied, and the fin height was kept constant. So, channel to fin height ratios (H_d/H_f) were varied from 2.0 to 5.0. The first row of fins was located 200 mm from the channel entrance. The

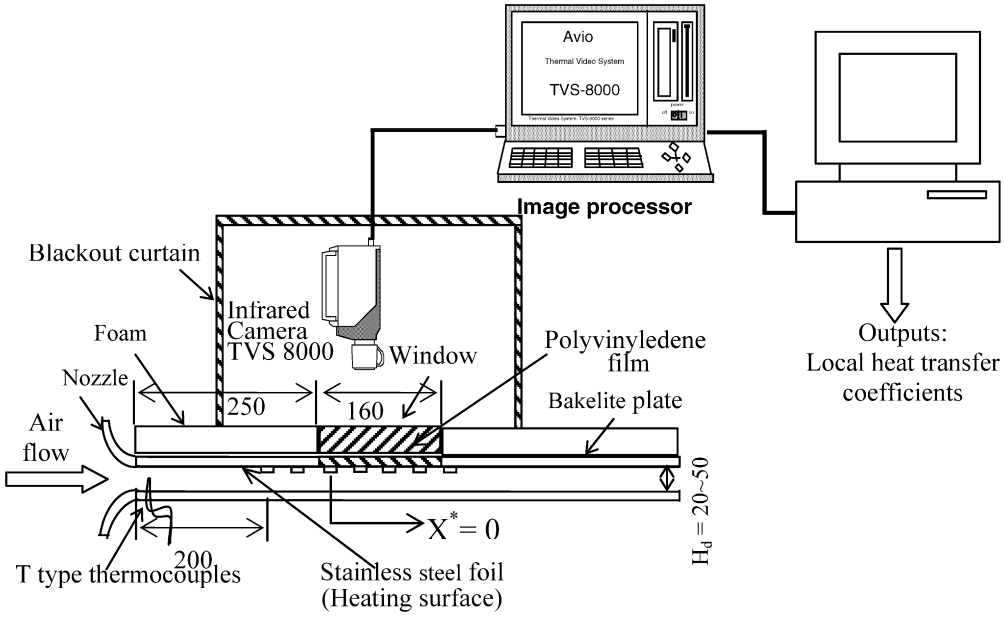

Fig. 1. Infrared image techniques.

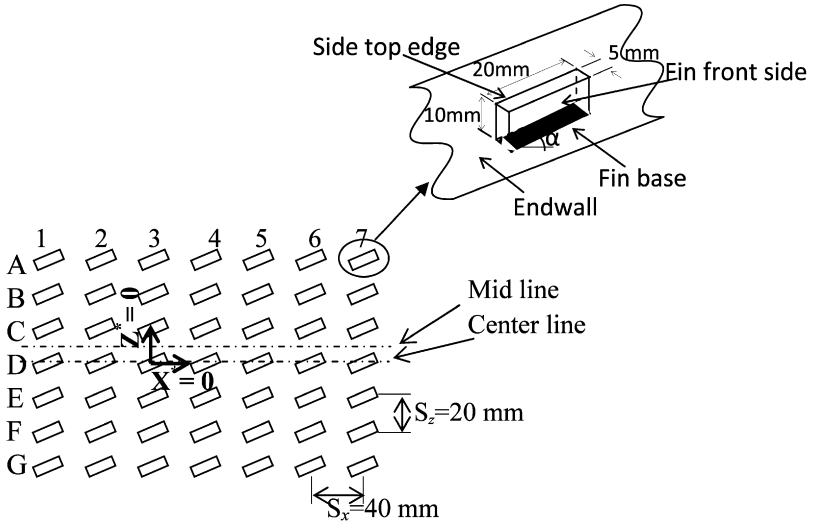

Fig. 2. Co-angular type fin pattern.

experimental apparatus with rectangular fins is shown in Fig. 1. The fins were made of aluminum and have rectangular dimensions of 20 mm (length) × 5 mm (thickness) × 10 mm (height). The fins were set in lines and rows of seven each. Fin spacing, fin center to center distance S_x, in streamwise direction were set to 40 mm whereas S_z in spanwise direction was 20 mm as shown in Fig. 2. The ratios S_x/L and S_z/L are defined as pitch ratio. Aspect ratio of the channel can be defined as the ratio of channel height to channel width. Geometrical specification of test channels is shown in Table 1. The inclination angle of the fins with respect to the flow direction was fixed at $\alpha = 20°$. The fins were attached to the inner side of the upper plate of the channel by means of a 100 μm double sided thin tape. Since the tape electrically insulated the fin (aluminum material) from stainless steel foil, no heat will be generated within these aluminum fins. At the same time, the tape has a very low thermal conductivity resistance compared with convective resistance of fins. Therefore, the heat generated in the stainless steel foil will flow to the aluminum fins by heat conduction process. A schematic figure of the co-angular fin pattern used in this study is illustrated in Fig. 2.

Table 1
Geometrical specification of test channels.

Width (W) (mm)	Height (H_d) (mm)	Hydraulic diameter (D_H) (mm)	Aspect ratio (H_d/W)	Channel height to fin height ratio (H_d/H_f)	Fin height to hydraulic diameter ratio (H_f/D_H)
230	20	40	0.086	2	0.25
230	25	50	0.108	2.5	0.2
230	30	60	0.130	3	0.166
230	35	70	0.152	3.5	0.142
230	40	80	0.174	4	0.125
230	45	90	0.195	4.5	0.111
230	50	100	0.5	5	0.10

To measure the pressure drop resulting from the presence of the fins, 0.5 mm diameter static pressure taps were placed at 13 locations upstream and downstream from the fins on the pressure plate at 60–120 mm intervals. To measure the local heat transfer coefficients, the channel wall was formed from a 10 mm thick bakelite plate with a 30 μm thick stainless steel foil heating surface. During the experiment, the temperature difference between

Table 2
Calculated bulk temperature at exit from the energy balance for all channel aspect ratios and air velocity.

Aspect ratio (H_d/W)	$U = 3$ m/s		$U = 4$ m/s		$U = 5$ m/s		$U = 6$ m/s		$U = 7$ m/s		$U = 8$ m/s		$U = 10$ m/s	
	T_{inlet} (°C)	T_{exit} (°C)	T_{inlet} (°C)	T_{exit} (°C)	T_{inlet} (°C)	T_{exit} (°C)	T_{inlet} (°C)	T_{exit} (°C)	T_{inlet} (°C)	T_{exit} (°C)	T_{inlet} (°C)	T_{exit} (°C)	T_{inlet} (°C)	T_{exit} (°C)
0.086	32.41	38.89	32.9	38.52	33.2	38.41	33.35	38.14	33.51	38.12	33.71	38.25	33.97	38.22
0.108	32.82	37.33	33.15	37.06	33.35	37.07	33.58	37.18	33.81	37.16	33.94	37.11	34.22	37.26
0.130	33.3	36.82	33.86	36.90	34.17	37.14	34.63	37.38	34.88	37.49	35.06	37.66	35.60	38.09
0.152	33.38	36.24	33.64	36.25	33.86	36.35	33.96	36.37	34.09	36.29	34.43	36.60	34.43	36.57
0.174	32.51	35.01	32.89	35.13	33.28	35.36	33.46	35.42	33.66	35.59	33.74	35.58	33.94	35.69
0.195	32.39	34.49	32.64	34.58	32.39	34.30	32.69	34.42	32.89	34.54	33	34.61	33.15	34.75
0.5	32.23	34.13	32.54	34.19	32.82	34.45	33.07	34.61	33.17	34.61	33.28	34.67	33.48	34.80

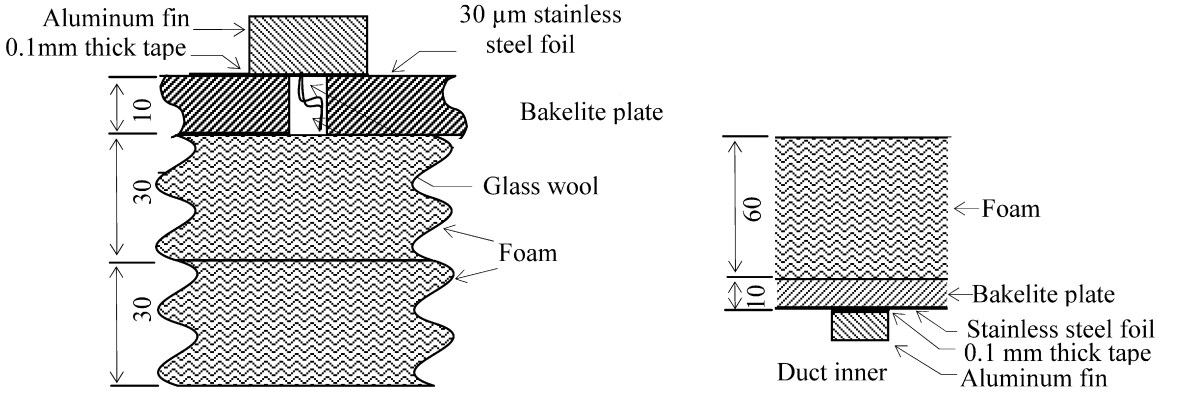

(a) Thermal insulation of the heating surface attached with thermocouples. (b) Thermal insulation of the heating surface except window

Fig. 3. Thermal insulation techniques.

mainstream and the heating surface was kept constant and the heat flux was varied. It should be mentioned that the temperature difference between mainstream and heated wall at one particular spot was monitored by adjusting the heat flux in the heating surface. The mainstream temperature was calculated by averaging the temperatures of the two T-type thermocouples located at the middle of the channel height as shown in Fig. 1. Bulk temperature at the exit of the channel for different channel aspect ratio and air velocity are also calculated from the energy balance equation and is shown in Table 2. To prevent heat loss from the heating surface, the bakelite plate was insulated by a layer of 50 mm thick foam except for the window area through which the infrared image was taken as shown in Fig. 3. The infrared image technique was employed in order to observe the temperature distributions and the heat transfer coefficients on the overall surface including the fin base and endwall. Images were taken using an infrared camera with an indium-antimony (In-Sb) sensor, which can measure the temperature at 160×120 points with a resolution of 0.025 °C for a black body. In this case, the temperature was measured at the back of the heating surface through a window (80 mm × 160 mm) which was covered by polyvinyledene film with a transmissivity for infrared energy of nearly unity. The back of the heating surface was painted black and the whole experimental apparatus was covered by black cloth to ensure that the surroundings were completely dark. Since the fins are electrically insulated with having very low thermal contact resistance at the fin base, the wall temperature measurement of the back of the stainless steel foil through window will eventually reflect the temperature of the fin base and endwall (fin base excluded). A centrifugal (NIKO TPH) blower was used to supply the air in the channel. The blower specifications were: flow rate 45 m^3/min, pressure 350 mm Aq., power 5.5 kW and revolution 2830 rpm. The velocity profile at the inlet of the channel was uniform with a thin boundary layer and the turbulence intensity was 3% of the main flow velocity at the channel inlet. The detailed heat transfer and the averaged Nusselt number in the representative (window) region, especially at the third, fourth, fifth and sixth rows were estimated from the infrared images. The experiments were performed for Reynolds numbers in the range of $Re = 7500$–130000 ($U = 3$–10 m/s), based on the mainstream velocity and the hydraulic diameter of the channel (see Eq. (3)).

3. Data reduction

In this study, we investigated the heat transfer characteristics and fluid flow behavior. The essential quantities determined were the friction factor and the heat transfer coefficients for the co-angular fin pattern at various channel heights.

The total heat generated from the heating surface is distributed by convection to the flowing air, heat losses through the insulation and the window. It was found that the heat loss from window was 1.3% of the heat flux supplied to the heating surface. This value is so small compared to the heat input that it can be neglected. Consequently, the total heat transferred by convection to the flowing air equals the heat flux supplied to the heating surface.

The friction factor f was evaluated from the pressure difference between points just upstream and downstream of the fins attached to the heating surface using Eq. (1)

$$P_{loss} = f(l/D_H)(\rho_a U^2/2) \tag{1}$$

where l is the distance to the reference region, i.e. the distance between just upstream of the D1 fin and downstream of the $D7$ fin, D_H is the hydraulic diameter of the channel and P_{loss} is the total pressure drop due to the finned surface.

The heat transfer coefficients,

$$h = \dot{q}/(t_w - t_\infty) \tag{2}$$

were obtained in representative (window) region, where t_w is the wall temperature, t_∞ is the mainstream temperature and $\dot{q}$ is the heat flux per unit area of the heating surface.

Reynolds numbers is based on the mainstream velocity and the channel's hydraulic diameter, and can be expressed as

$$Re = U D_H/\nu \tag{3}$$

The area-averaged Nusselt number based on the channel's hydraulic diameter can be expressed as

$$\overline{Nu} = \bar{h} D_H/\lambda \tag{4}$$

4. Uncertainty analysis

The pressure was measured by a digital micro manometer with an accuracy of ±0.1 mm of H_2O. The heating surface was covered with 50 mm thick insulating foam to prevent heat loss from the heating surface. Therefore, heat losses from the back of the heating surface may be assumed to be very small. The window was covered with two layers of polyvinyledene film separated by 1 mm and heat losses were found to be 1.3% of the heat flux supplied to the surface. As a result, the heat transfer coefficient contained less than 3% uncertainty. The temperature was measured with the infrared camera, and the thermocouples using a data logger. The percentage relative uncertainty in the measured temperature for the thermocouples and the infrared camera were ±0.25% and ±1.3%, respectively. The percentage relative uncertainty in the measured electric power input was ±1.4%. The percentage relative uncertainty in the compound variables were found to be less than ±5% both for the velocity and the Reynolds number and ±3% both for the heat transfer coefficient and Nusselt number.

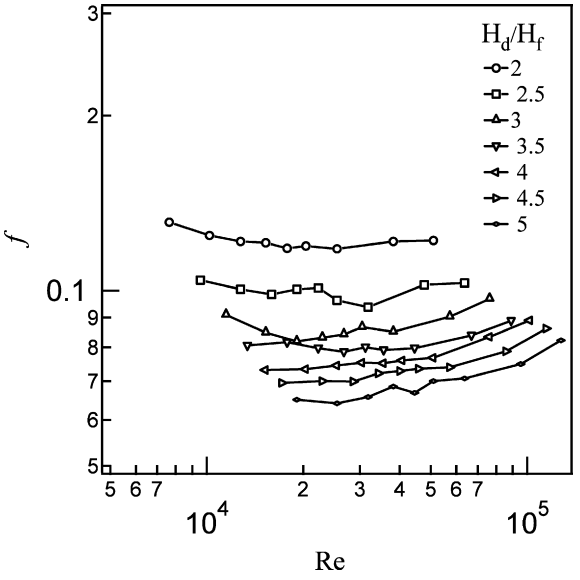

Fig. 4. Variation of friction factors with Reynolds numbers for co-angular pattern at different channel to fin height ratios.

5. Results and discussions

5.1. Friction factor

To estimate the pressure drop and the thermal performance with the insertion of the fins, the friction factors for different channel heights were measured, and the results are presented in Fig. 4. The friction factor f is obtained from Eq. (1). The friction factor decreases with an increase of the channel to fin height ratio (H_d/H_f). This trend is expected because larger friction occurs for smaller channel to fin height ratios. This friction occurs due to the turbulence and flow interactions caused by the co-angular pattern. There is a relatively large difference in the friction factors between the channel to fin height ratios (H_d/H_f) of 2 and 2.5. The friction factor slowly decreases with Reynolds number and this tendency continues for channel to fin height ratios of 2 and 2.5. For the other channel to fin height ratios, the friction factor initially decreases with increasing Reynolds number, but finally slowly increases with Reynolds number. At smaller channel to fin height ratios, the vortexes generated by the inclined fins are reflected by the lower wall that strongly touches the endwall and fin surfaces which increase the friction. On the other hand, at larger channel to fin height ratios, the lower wall has comparatively less influence on the vortex structure and the flow is not reflected strongly by the wall as well. So less friction is experienced. At higher Reynolds number, inclined fins cause a complex flow structure as well as larger flow interactions with fins and endwall. As a result, large pressure drops are experienced and friction factors are slightly increased at higher Reynolds number.

5.2. Detailed heat transfer analysis

5.2.1. Detailed heat transfer

The observed influence of channel to fin height ratios on heat transfer coefficient profile and iso-heat transfer coefficient contour is observed which is shown in Fig. 5. The channel to fin height ratios increases from 2 (a) to 5 (g). Channel aspect ratio and Reynolds number as well as mass flow rates are also mentioned in the figures which are found increasing with H_d/H_f. Table 3

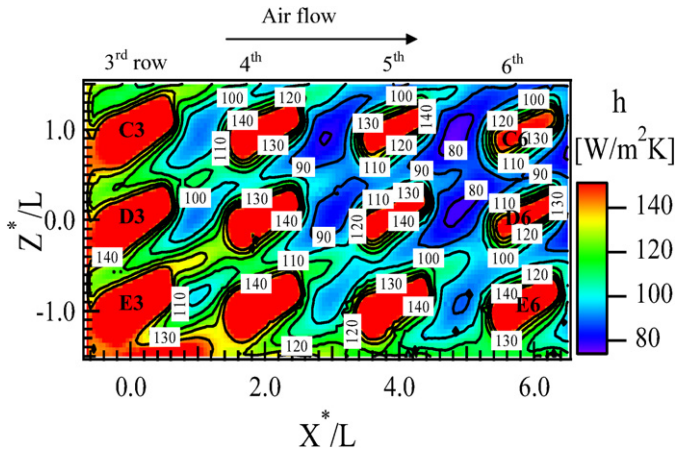

(a) $H_d/W = 0.086$, $H_f/D_H = 0.25$, $Re = 25494$, $\dot{m} = 0.054$ kg/s

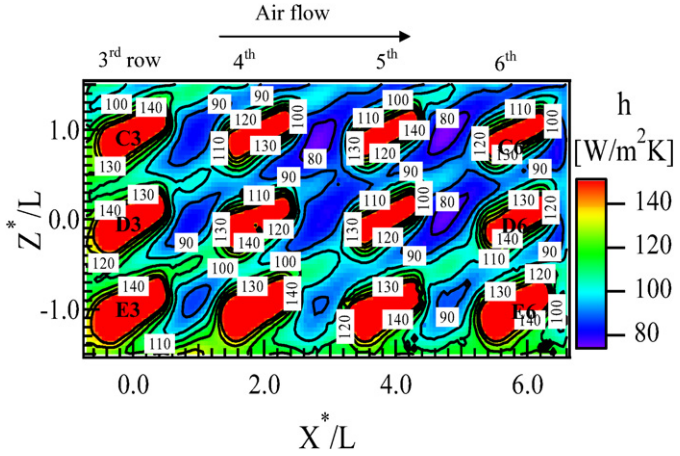

(b) $H_d/W = 0.108$, $H_f/D_H = 0.2$, $Re = 31867$, $\dot{m} = 0.067$ kg/s

Fig. 5. Detailed heat transfer coefficient profile with iso-heat transfer coefficient contour of the representative fin region with co-angular pattern for $U = 10$ m/s and for channel to fin height ratios of (a) 2, (b) 2.5, (c) 3, (d) 3.5, (e) 4, (f) 4.5 and (g) 5.

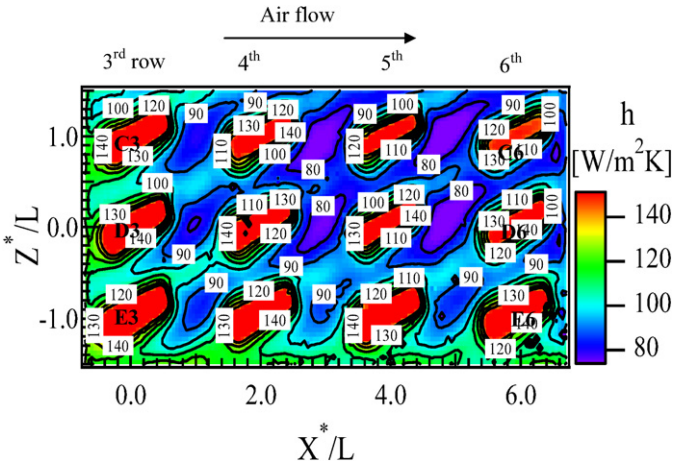

(c) $H_d/W = 0.130$, $H_f/D_H = 0.166$, $Re = 38241$, $\dot{m} = 0.081$ kg/s

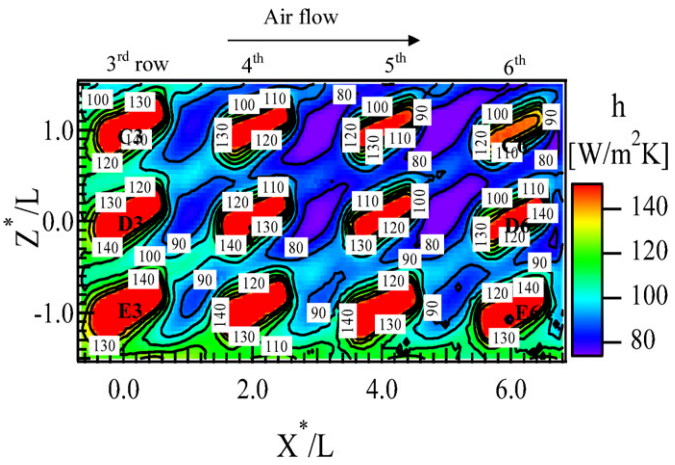

(d) $H_d/W = 0.152$, $H_f/D_H = 0.142$, $Re = 44614$, $\dot{m} = 0.094$ kg/s

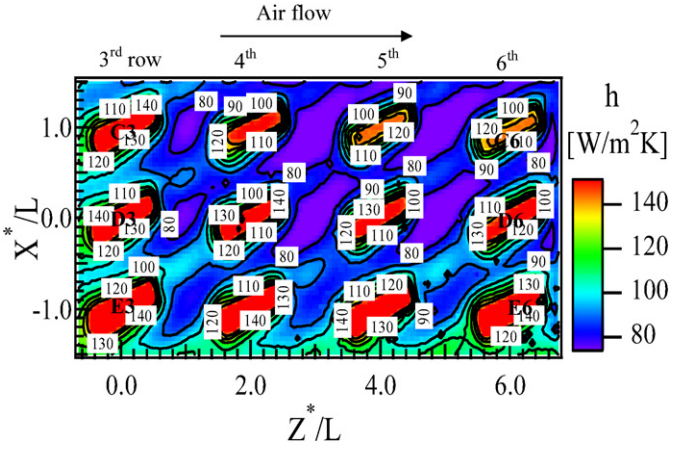

(e) $H_d/W = 0.174$, $H_f/D_H = 0.125$, $Re = 50988$, $\dot{m} = 0.108$ kg/s

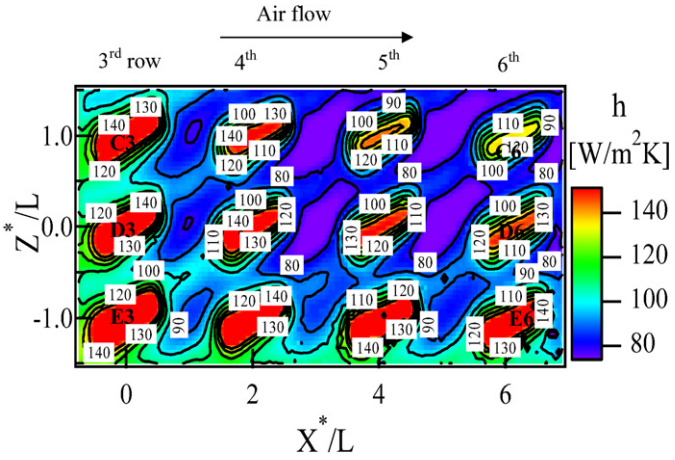

(f) $H_d/W = 0.195$, $H_f/D_H = 0.111$, $Re = 57361$, $\dot{m} = 0.121$ kg/s

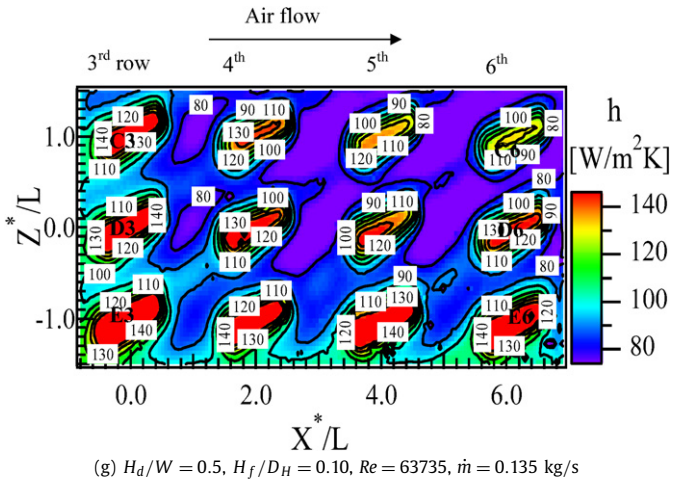

(g) $H_d/W = 0.5$, $H_f/D_H = 0.10$, $Re = 63735$, $\dot{m} = 0.135$ kg/s

Fig. 5. (*Continued*)

Table 3
Mass flow rate of air for different channel aspect ratio and air velocity.

Aspect ratio (H_d/W)	Mass flow rate, $\dot{m}$ kg/s						
	3 m/s	4 m/s	5 m/s	6 m/s	7 m/s	8 m/s	10 m/s
0.108	0.020303	0.027071	0.033839	0.040607	0.047374	0.054142	0.0676775
0.130	0.024364	0.032485	0.040607	0.048728	0.056849	0.06497	0.081213
0.152	0.028425	0.037899	0.047374	0.056849	0.066324	0.075799	0.0947485
0.174	0.032485	0.043314	0.054142	0.06497	0.075799	0.086627	0.108284
0.195	0.036546	0.048728	0.06091	0.073092	0.085274	0.097456	0.1218195
0.5	0.040607	0.054142	0.067678	0.081213	0.094749	0.108284	0.135355

shows the mass flow rates for different channel aspect ratio and air velocity. We can compare the heat transfer coefficient contour from Fig. 5 (a)–(g), because the range of heat transfer coefficients is kept the same for all of the figures. Though the shape of the iso-heat transfer coefficient contour of the fin rows on the endwall is found to be similar regardless of the channel to fin height ratio and aspect ratio of the channel, the areas of higher heat transfer and lower heat transfer are clearly different on the endwall. In Fig. 5, it is observed that the higher heat transfer region decreases in area with increasing channel to fin height ratio (H_d/H_f) and aspect ratio (H_d/W) of the channel as well. The higher heat transfer regions adjacent to the fin base also decrease with increasing channel to fin height ratio and aspect ratio of the channel. The iso-heat transfer coefficient contour also shows the enlarged area of higher heat transfer on the endwall in the case of lower channel to fin height ratio, while the lower heat transfer regions apparently enlarge with increasing channel to fin height ratio. In this fin arrangement, longitudinal vortex generated by inclined fins strikes the inter-fin region and the following fin surfaces strongly and so the extended surface effect is higher. At the same time, formation of horse shoe vortex [2] at the front of the fins is another reason for heat transfer enhancement in that particular region. This

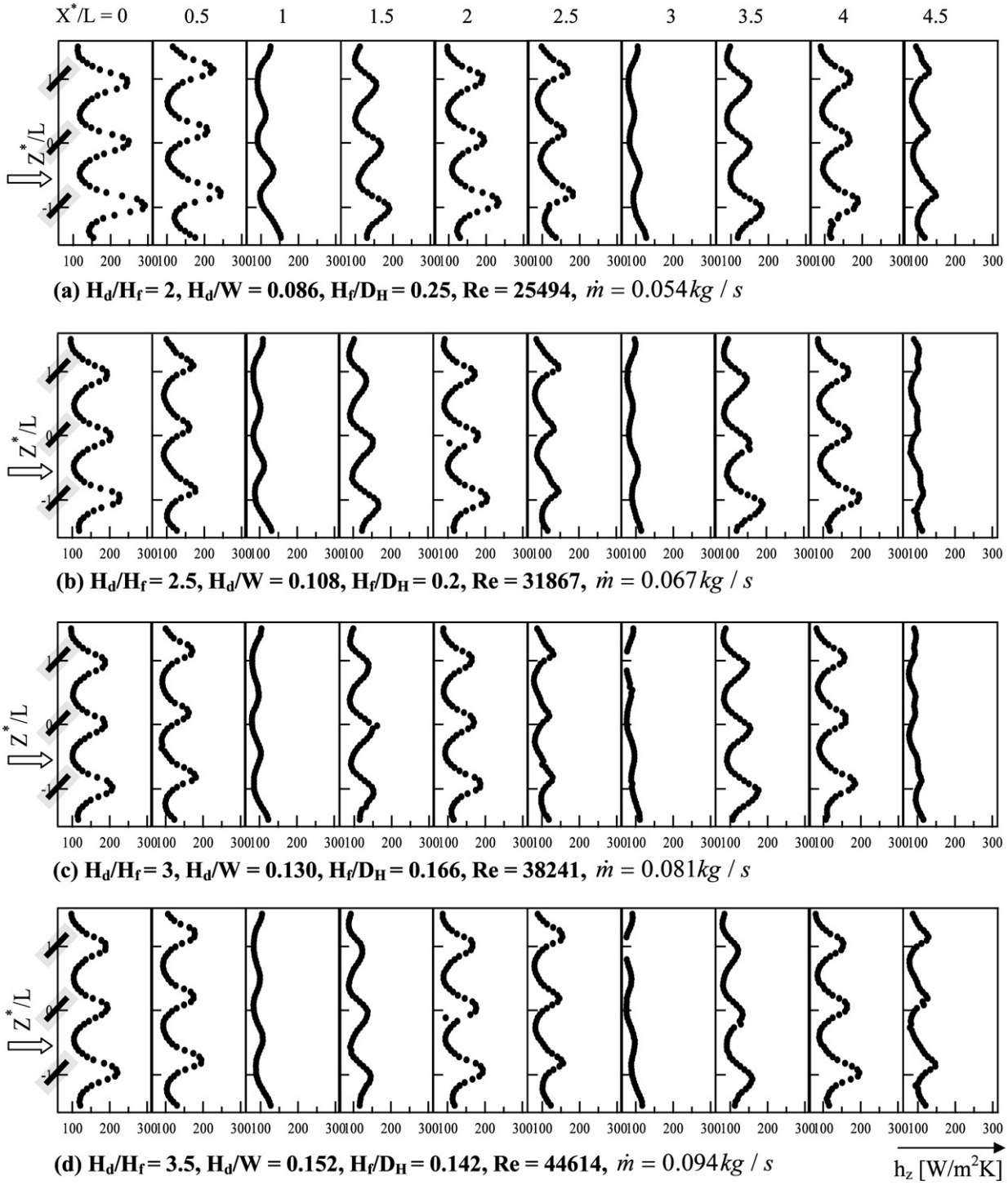

Fig. 6. Spanwise heat transfer coefficient distributions on the endwall for $U = 10$ m/s in different channel to fin height ratios.

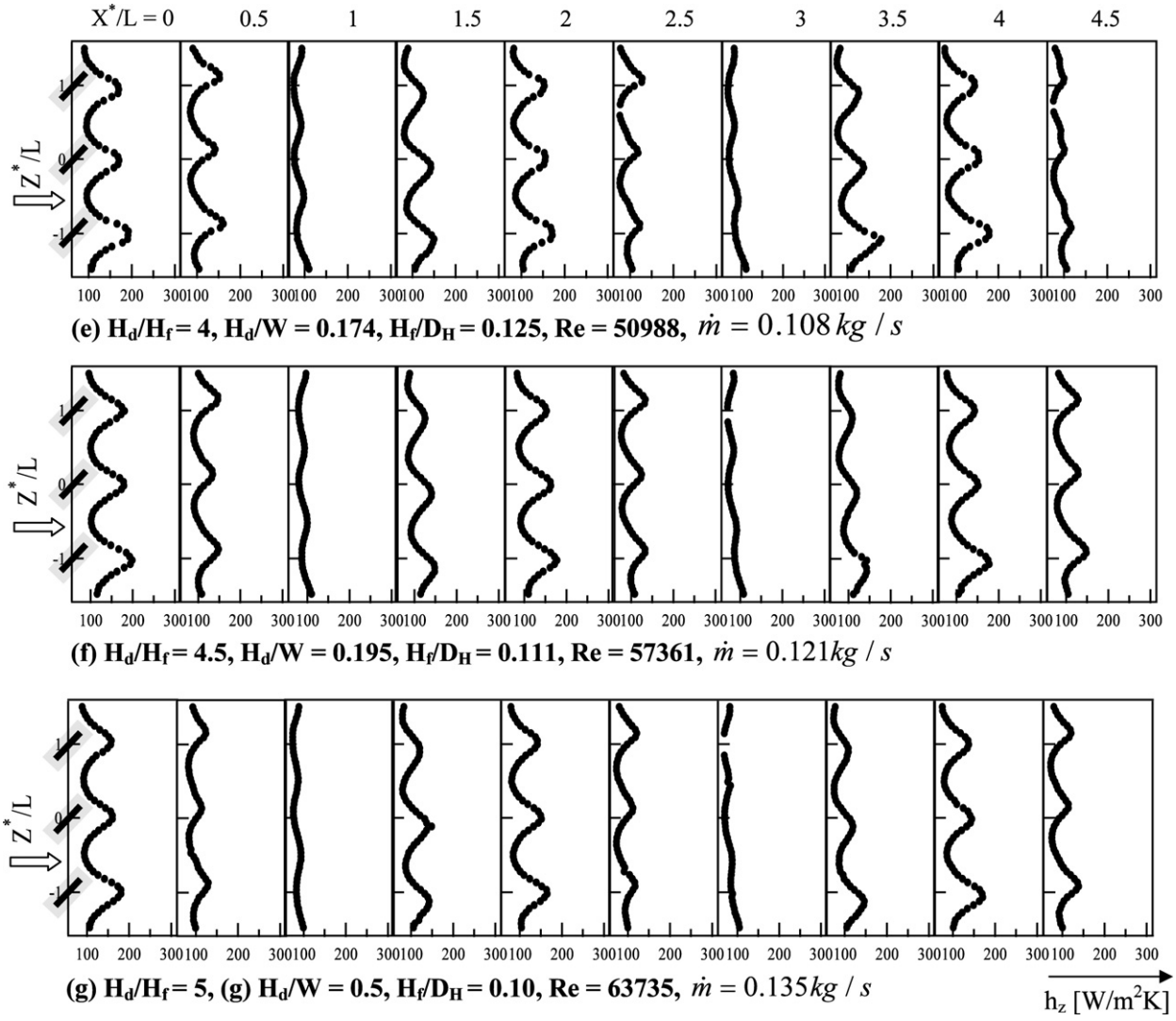

Fig. 6. (*Continued*)

flow behavior is clearly explained by flow visualization around the co-angular fins [1]. At a smaller H_d/H_f and H_d/W, both strength and circulation of the longitudinal vortex are affected by the lower wall of the channel. The separation space between lower wall and fin top edge has a significant role in the phenomena of flow separated from the fin top edge, vortex structure and vortex circulation. In case of large H_d/H_f and H_d/W, separation space has less impact on the vortex structure and circulation. As a result, the heat transfer characteristics change with channel to fin height ratios and channel aspect ratios. The iso-heat transfer contour and heat transfer profile also show that the heat transfer coefficients decrease with increasing channel to fin height ratio. The channel to fin height ratio of 2, i.e. 20 mm channel has the highest heat transfer among the heights tested.

In order to understand the heat transfer distributions more clearly, spanwise heat transfer distributions are drawn at some streamwise locations for the representative fin region. In Fig. 6 spanwise heat transfer distributions are shown for all channels to fin height ratios (H_d/H_f) and channel aspect ratio (H_d/W). Fin locations are also shown in the figures to get the relation between flow physics and the heat transfer characteristics. At the fin centers, i.e. along $X^*/L = 0$, 2 and 4, the spanwise heat transfer distributions are periodic. Peak values are found at the fin centers and the trough values are located between the fins in the spanwise direction, i.e. at $Z^*/L = +0.5$ and -0.5. The highest heat transfer coefficient at the fin center position is due to combined effect of extended surface and vortex generator. For all cases, peak values are sharper than the trough values. This sharpness decreases with increasing the channel to fin height ratios and the heat transfer coefficient of the peak values gradually decrease along the streamwise direction for all cases. Just behind the fins, i.e. at $X^*/L = 0.5$, 2.5 and 4.5, a periodic distribution appears, but it is remarkable that the trough values are somewhat larger than the corresponding locations at the fin centerline. This is expected because the vortex generated by inclined fin touches the endwall (base plate) just after the fins [2]. At the middle of the fin rows, i.e. $X^*/L = 1$ and 3, the shape of the profile is not distinctly periodic. At the front of the fins, the heat transfer profile becomes periodic again. Fig. 6 also shows that the heat transfer coefficient profile in the streamwise direction remains similar for all channels to fin height ratio but with some differences in value.

5.3. Area averaged heat transfer coefficient and Nusselt numbers

We have estimated the area averaged heat transfer coefficient of the endwall with and without fin base of the representative fin region for different channel to fin height ratios and aspect ratios. Then we calculated the average Nusselt number based on the hydraulic diameter of the channel and the average heat transfer

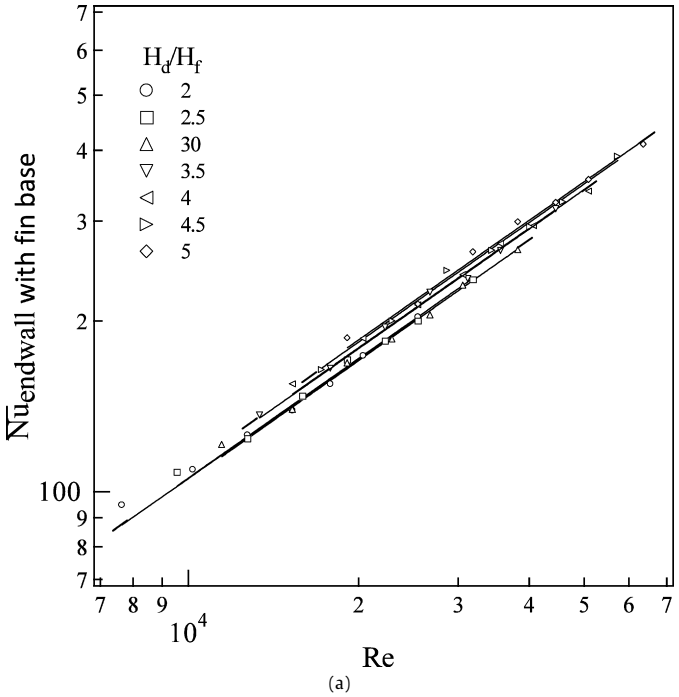

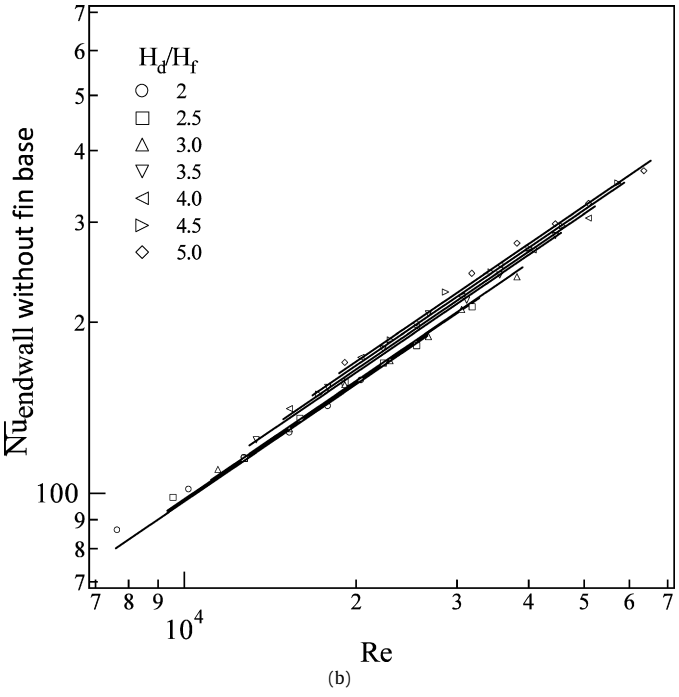

Fig. 7. Relationship between Nusselt number and Reynolds number for (a) the endwall with fin base and (b) the end wall without fin base (flat portion only).

coefficient. The relationship between the Nusselt number and the Reynolds number for different channel to fin height ratios as well as aspect ratios is shown in Fig. 7. Fig. 7(a) shows the area averaged Nusselt number for the endwall with fin base whereas the area averaged Nusselt number of the endwall without fin base (flat portion only) is shown in Fig. 7(b). Here, H_d/H_f ratio alters the H_d/W ratio and the channel hydraulic diameter. Since the Nusselt number is based on the channel's hydraulic diameter, Nusselt values increase with channel height regardless of Reynolds number. As shown in Fig. 7 (a) and (b), there is no significant difference in Nusselt values between the different channels to fin height ratios.

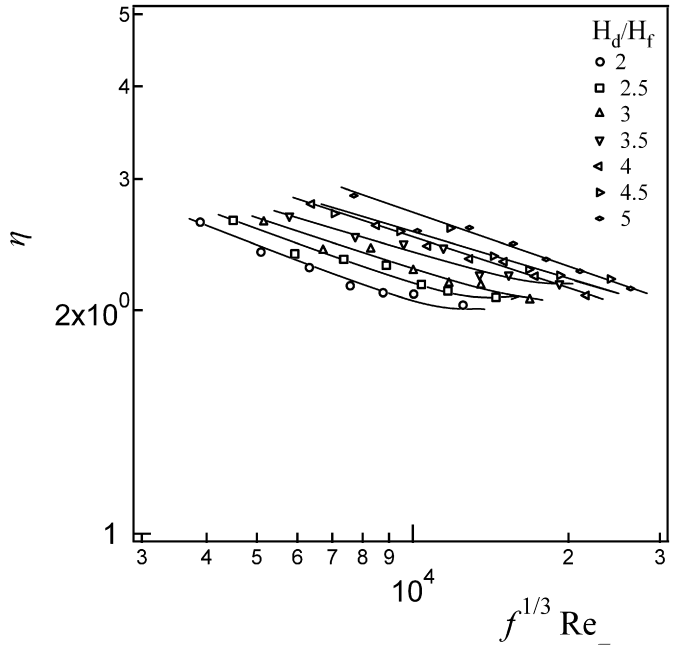

Fig. 8. Thermal performance ratios with Reynolds number for different channel to fin height ratios.

5.4. Thermal performance ratio

Various techniques may be proposed for evaluating the thermal performance ratio depending on the purpose for which a heat exchanger is designed [19]. Here the heat transfer enhancement rate will be evaluated for the promoter case, keeping the pumping power and heat transfer area constant. In this case, the relationship between Re and Re_s, at the smooth surface, can be derived from the limiting condition and written as [20],

$$Re_s = Re(f/f_s)^{1/3} \tag{5}$$

Where, f_s is the friction factor at the smooth surface. Substituting $f_s = 0.3164Re_s^{-1/4}$ into Eq. (5) yields

$$Re_s = (fRe^3/0.3164)^{1/2.75}$$

Finding Nu_s for Re_s, we have the heat transfer augmentation rate

$$\eta = \overline{h_x}/h_s = \overline{Nu}/Nu_s \tag{6}$$

Eq. (6) indicates that there will be a net energy gain only if η is greater than unity. In Fig. 8, the relationship between thermal performance ratios and Reynolds numbers is shown. Thermal performance decreases with Reynolds number regardless of the channel to fin height ratio and channel aspect ratios. In general, it is seen that η has higher values for all channel to fin height ratios and aspect ratios in the lower regime of $f^{1/3}Re$, and its value reaches nearly 3. The differences in the thermal performance ratios for different H_d/H_f are almost equal. Next, we investigate the effect of channel to fin height ratio on thermal performance and find the optimal channel height by comparison with a reference channel height. The following relation is obtained under the constant pumping power condition, where a reference channel is expressed with subindex "ref":

$$f^{1/3}Re(H_{\text{dref}}/H_d) = f^{1/3}Re_{\text{ref}} \tag{7}$$

where H_{dref} denotes a reference channel height. The heat transfer augmentation or thermal performance ratio $\acute{\eta}$ is then expressed as follows:

$$\acute{\eta} = \bar{h}/\bar{h}_{\text{ref}} \tag{8}$$

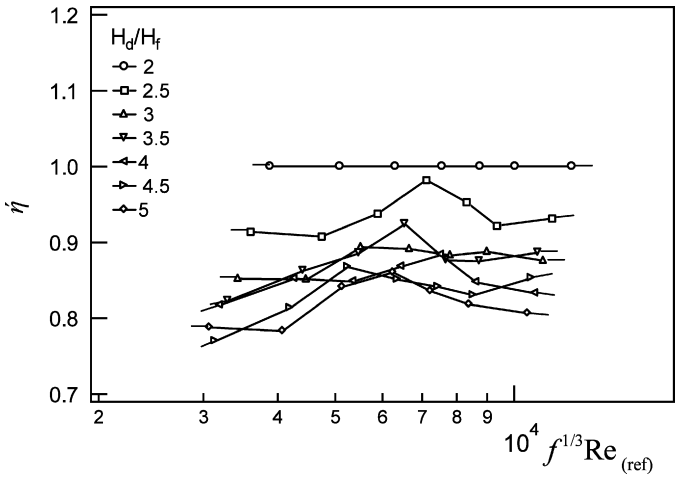

Fig. 9. Effect of channel to fin height ratios on the relative performance evaluation.

We select $H_d = 20$ mm as the reference channel height, the data for relative performance ratio $\acute{\eta}$ based on Eq. (8) is shown as a function $f^{1/3}Re_{\mathrm{ref}}$ in Fig. 9.

From the relative performance graph it is clear that $H_d/H_f = 2$ have the highest thermal performance amongst the channel to fin height ratios tested. Additionally, it is found that thermal performance decreases with increasing the channel to fin height ratios and the channel aspect ratios. This is explained earlier that at smaller H_d/H_f and H_d/W, the separation space has a significant effect on vortex strength and structure which causes larger flow interaction with fin surfaces and endwall and leads to a higher heat transfer enhancement.

6. Conclusions

We have experimentally investigated the effects of channel height on heat transfer enhancement on the overall surface with short rectangular plates of a co-angular type pattern in the rectangular channel in order to develop high performance heat exchangers. After a thorough investigation we summarize the results as follows:

(1) The iso-heat transfer coefficient profile and the detailed heat transfer distributions give a clear picture of how the channel height influences the heat transfer from the endwall. Iso-heat transfer contour and spanwise distributions clearly indicates that higher heat transfer areas are comparatively larger for the smaller H_d/H_f and H_d/W than that of the larger H_d/H_f and H_d/W. Heat transfer at the fin base and in inter-fin space in streamwise decreases with larger H_d/H_f and H_d/W. This is due to the influence of the separation space between lower wall and fin top edge.

(2) The Nusselt number increases with the Reynolds number regardless of channel to fin height ratio.

(3) The relative performance graph shows that the highest thermal performance could be achieve at the smallest channel to fin height ratio ($H_d/H_f = 2$) and smallest aspect ratio ($H_d/W = 0.086$). It is also found that the thermal performance decreases with increasing the channel to fin height ratio and aspect ratio.

(4) At low Reynolds number, the thermal performance can be increased 2.6–3 times relative to the smooth surface depending on the channel to fin height ratio and channel aspect ratios.

(5) For the channel to fin height ratios of 2 and 2.5, the friction factor slowly decreases with Reynolds number. For the other cases, the friction factor initially decreases but finally increases with Reynolds number due to the complex flow phenomena at larger Reynolds number.

Acknowledgements

This research work is partially supported by the Heiwa Nakajima Foundation (HNF) of Tokyo, Japan. This support is gratefully acknowledged. I am also grateful to The Petroleum Institute, Abu Dhabi, UAE for their present support.

References

[1] M.D. Islam, K. Oyakawa, M. Yaga, Enhancement of heat transfer from a surface with rectangular fins of different patters and arrangements in a duct flow, Journal of Enhanced Heat Transfer 15 (1) (2008) 31–50.
[2] M.D. Islam, K. Oyakawa, M. Yaga, I. Senaha, Study on heat transfer and fluid flow characteristics with short rectangular plate fin of different pattern, Experimental Thermal and Fluid Science 31 (4) (2007) 367–379.
[3] K. Oyakawa, M.D. Islam, M. Yaga, Fluid flow and infrared image analysis on endwall fitted with short rectangular plate fin, Journal of Thermal Science 15 (2) (2006) 145–151.
[4] E.M. Sparrow, J.E. Niethammer, A. Chaboki, Heat transfer and pressure drop characteristics of arrays of rectangular modules encountered in electronic equipment, Int. J. Heat Mass Transfer 25 (1982) 961–973.
[5] E.M. Sparrow, S.B. Vemuri, D.S. Kadle, Enhanced and local heat transfer, pressure drop, and flow visualization for arrays of block-like electronic components, Int. J. Heat Mass Transfer 26 (1983) 689–699.
[6] M. Molki, M. Faghri, O. Ozbay, A correlation for heat transfer and wake effect in the entrance region of an inline array of rectangular blocks simulating electronic components, ASME Journal of Heat Transfer 117 (1995) 40–46.
[7] D.S. Kadle, E.M. Sparrow, Numerical and experimental study of turbulent heat transfer and fluid flow in longitudinal fin array, ASME J. Heat Transfer 108 (1986) 16–23.
[8] A.Y. Turk, G.H. Junkhan, Heat transfer enhancement downstream of vortex generators on a flat plate, in: C.L. Tien, V.P. Carey, J.K. Ferrell (Eds.), Heat Transfer, vol. 6, Hemisphere, Washington, 1986, pp. 2903–2908.
[9] S.A. El-Saed, S.M. Mohamed, A.M. Abdel-Latif, A.E. Abouda, Investigation of turbulent heat transfer and fluid flow in longitudinal rectangular fin-arrays of different geometries and shrouded fin array, Experimental Thermal and Fluid Science 26 (2002) 879–900.
[10] K. Oyakawa, Y. Furukawa, T. Taira, I. Senaha, Effect of vortex generators on heat transfer enhancement in a duct, in: Proceeding of the Experimental Heat Transfer, Fluid Mechanics and Thermodynamics, Honolulu, Hawaii, 31 October–November 5, vol. 1, 1993, pp. 633–640.
[11] T. Igarashi, Local heat transfer from a square prism to an air stream, Int. J. Heat Mass Transfer 29 (5) (1983) 777–784.
[12] K. Bilen, S. Yapici, Heat transfer from a surface fitted with rectangular blocks at different orientation angle, Heat and Mass Transfer 38 (2002) 649–655.
[13] J.S. Park, J.C. Han, Y. Huang, S. Ou, R.J. Boyle, Heat transfer performance comparisons of five different rectangular channels with parallel angled ribs, Int. J. Heat Mass Transfer 35 (11) (1992) 2891–2903.
[14] G.R. Warrier, V.K. Dhir, L.A. Momoda, Heat transfer and pressure drop in narrow rectangular channel, Experimental Thermal and Fluid Science 26 (1) (2002) 53–63.
[15] C. Mingoo, C. Keumnam, Effect of the aspect ratio of rectangular channels on the heat transfer and hydrodynamics of paraffin slurry flow, Int. J. Heat Mass Transfer 44 (1) (2001) 55–61.
[16] S.W. Chang, T.L. Yang, R.F. Huang, K.C. Sung, Influence of channel-height on heat transfer in rectangular channels with skewed ribs at different bleed conditions, Int. J. Heat Mass Transfer 50 (23–24) (2007) 4581–4599.
[17] S.W. Chang, T.M. Liou, M.H. Lu, Heat transfer of rectangular narrow channel with two opposite scale-roughened walls, Int. J. Heat Mass Transfer 48 (19–20) (2005) 3921–3931.
[18] A. Murata, S. Mochizuki, Effect of cross-sectional aspect ratio on turbulent heat transfer in an orthogonally rotating rectangular duct with angled rib turbulators, Int. J. Heat Mass Transfer 46 (16) (2003) 3119–3133.
[19] A.E. Bergles, A.R. Blumenkrantz, J. Taborek, Performance evaluation criteria for enhanced heat transfer surfaces, in: Proc. 5th Internat. Heat Trans. Conf., Tokyo, vol. 2, 1974, pp. 234–239.
[20] R.L. Webb, E.R.G. Eckert, Application of rough surfaces to heat transfer exchanger design, Int. J. Heat Mass Transfer (15) (1972) 1647–1657.